A Simplified Finite Element Analysis Method for Axial Compression Behavior of Rectangular Concrete Columns with Interlocking Multi-spiral Reinforcements

Ping-Hsiung Wang[1][a] and Kuo-Chun Chang[2][b]
[1]National Center for Research on Earthquake Engineering, Taipei, Taiwan
[2]Department of Civil Engineering, National Taiwan University, Taipei, Taiwan

Abstract: This paper proposes a simplified finite element analysis method to analyze the axial compression behavior of rectangular concrete columns confined by interlocking multi-spiral reinforcements. The proposed method utilizes an elastic finite element analysis to approximate the distribution and ultimate state of confining stress in each core concrete element, which is substituted into the Mander confined concrete model to obtain the integrated compressive curve of a column. Verification of the proposed method against the test results of four 4-spiral and four 5-spiral reinforcement columns shows good agreement. Parametric studies focused on the 5-spiral reinforcement show that for the same amount of transverse reinforcement, a column with a larger confined area, which closely depends on the radius ratio between the small and large spirals (r_s/r_b), can receive a better axial load-carrying capacity and confinement efficiency. To achieve economic confinement design, the volumetric ratio of large spirals to small spirals (ρ_s/ρ_b) to have the concurrent yielding of both large and small spirals was found to be around 1.0, 0.8, and 0.7 for r_s/r_b= 1/2, 1/3, and 1/4, respectively.

1 INTRODUCTION

Using confinement by transverse reinforcement, concrete columns can exhibit good ductile behavior and enhanced strength under axial compression. The efficiency of the confinement effect is dependent on the configuration of the confining steel as the effect is triggered passively with the lateral expansion of the confined concrete core. To fit the shape of the column section, tie reinforcements are generally used in rectangular columns while spirals or circular hoops are applied to circular columns. It is well recognized that the tie reinforcement is less efficient than the spiral or circular hoop, since the arching action of the former forms vertically between the levels of transverse steels and also horizontally between the tied longitudinal bars, resulting in more uneven confining stress than the latter. The current seismic design code (ACI 318-14 2014; Caltrans 2003) also requires less transverse reinforcements for spiral or circular hoop columns than for rectangular tied columns if the shear strength does not govern the column design.

To utilize the advantages of spiral confinement and to boost the fabrication automation of steel cages in the prefabrication industry, Yin et al., (2011; 2012) and Wang (2004) proposed using innovative interlocking multi-spiral as transverse reinforcements in rectangular concrete columns. Fig. 1 shows the axial stress-strain curves of two representative multi-spiral columns in comparison with those of a typical tied column (T1). In the figure, column 4S1 is comprised of four identical spirals, each of which interlocks with the others, while column 5S3 has one large spiral interlocking with four small ones at the corners of the column. It can be clearly seen that, based on approximately the same amount of transverse reinforcements, columns 4S1 and 5S3 show superior ductile behavior at the post-peak branch and their compressive strength can be increased by 19% and 28% compared to column T1, respectively.

A number of stress-strain constitutive models had

---

been developed for predicting the uniaxial compression behavior of confined and unconfined concrete (Sheikh and Uzumeri 1982; Mander et al., 1988; Saatcioglu and Razvi 1992; Cusson and Paultre, 1995; Hoshikuma et al., 1997). These models were empirically constructed based on experimental results and some simple analytical calculation; the key point of the models is to evaluate the effective confining pressure acting on the confined concrete core. For columns with irregular confinement configurations such as the interlocking multi-spiral mentioned above, however, the applicability of these models is limited due to the complicated distribution of confining pressure that cannot be computed by means of simple force equilibrium on confined units. In addition to the empirical models, the nonlinear finite element method is an alternative to simulating the confined behavior of concrete in a more detailed manner. Many finite element modeling methodologies have been developed (Karabinis and Kiousis, 1994; Malvar et al., 2004; Luccioni and Rougier, 2005; Papanikolaou and Kappos, 2009; Yu et al., 2010; Song and Lu, 2011; Teng et al., 2015) where the concrete plasticity constitutive model used plays a crucial role in affecting the reliability and accuracy of results. According to the complexity of the confining mechanism, different levels of sophistication may be required when defining the yield criterion, the strain hardening and softening rules, the flow rule, and even the damage function while many relevant parameters need to be calibrated. In general, compared to the experimental results, a circular concrete section with uniform confining stress provided by active pressure or fiber reinforced polymer (FRP) could result in better simulations, whereas a rectangular section confined by commonly used tie reinforcements would result in less favorable results. Nevertheless, no attempt has been made to apply these methodologies to rectangular multi-spiral columns and it can be expected to be a challenge.

The objective of this research was to propose a simplified finite element analysis method for analyzing the uniaxial compression behavior of rectangular concrete columns with complicated confinement configurations such as the interlocking 4-spiral and 5-spiral configurations mentioned above. The proposed method combined an elastic finite element analysis with an empirical stress-strain model of confined concrete to achieve efficient and satisfactory simulation results. Due to the superior confined behavior and favorable assembling automation, a parametric study focused on the interlocking 5-spiral was then used to evaluate the influence of various design parameters on the confi-
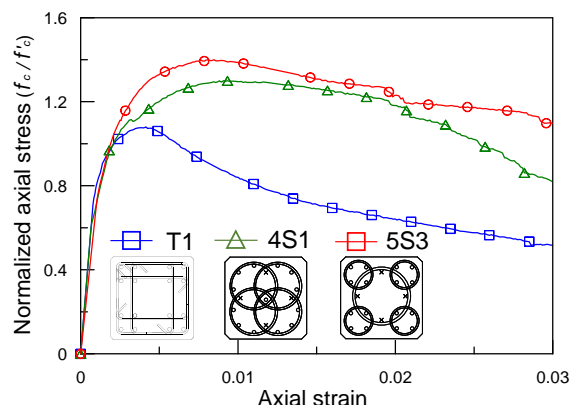
nement efficiency.

Figure 1: Comparison of axial compression behaviors of rectangular concrete columns with tie reinforcement and interlocking multi-spiral configurations.

2 FUNDAMENTAL CONCEPT AND ANALYTICAL PROCEDURE

The proposed simplified method made use of the advantages of both the empirical stress-strain confined concrete model and the finite element analysis method; the former could provide well established correlations between the effective confining stress and the confined concrete strength, while the latter could more realistically analyze the distribution of confining stress. The confined concrete model proposed by Mander et al., (1998) was used in the research. The key parameters of the Mander model are the effective confining stress f_l' for spiral (or circular hoop) reinforcement and the maximum (f_{l2}') and minimum (f_{l1}') effective confining stresses for rectangular tie reinforcement, all of which are exerted on the confined concrete core. The effective confining stress is further defined as a product of the confining stress f_l (or the maximum and minimum confining stresses, namely f_{l1} and f_{l2}, respectively) and the effective confinement coefficient k_e. Once these parameters are obtained, the stress-strain curve of confined concrete with enhanced compressive strength f_{cc}' and ductility can then be easily constructed. For columns with commonly used regular transverse reinforcements, the confining stress was approximated in the Mander model as uniformly distributed stress over the confined core using a simple force equilibrium. In addition, the effective confinement coefficient was assumed to be the ratio of the area of effectively

confined concrete core, which excludes the ineffectively confined area due to the arching action, to the area of confined concrete core enclosed by the perimeter of transverse reinforcement.

However, for interlocking multi-spiral columns, the inherently uneven and complicated distribution of confining stress cannot be approximated using the methodology mentioned above. Therefore, it was proposed in this research to derive the amount and distribution of confining stress by means of elastic finite element analysis. The proposed method was based on the assumption that the ultimate state of confining stress within the confined concrete core coincided with the maximum stress of confining steel that has just reached yielding stress. This may be justified by the fact that once the confining steel yields, the lateral expansion of confined concrete under axial compression cannot be effectively restrained, resulting in a significant increase in the Poisson's ratio of the concrete and a decrease in confining stress. With this assumption, elastic finite element analysis was used to approximate the ultimate state of confining stress, which can avoid nonlinear analysis, eliminating the need for sophisticated concrete plasticity modeling and time-consuming computation. Moreover, discrete circular hoops are used to simulate a continuous spiral for simplicity of modeling and calculation. The proposed method can be achieved as illustrated in Fig. 2 by firstly performing an elastic finite element analysis to impose a small amount of compressive displacement on the built model. Then, the maximum tensile stress of the confining steel f_{s_max} can be determined, and a horizontal layer of concrete elements between the level of confining steel having the maximum stress and its adjacent level can be selected for further calculation. The position of the selected layer of the concrete element is generally located at around the mid-height of the column due to the geometric symmetry and boundary constraints of the column, causing this location to have the largest lateral expansion as observed in experiments (Yin et al. 2011, 2012; Wang 2004). Second, the maximum and minimum confining (or principal) stresses of each confined concrete element of the selected layer are extracted from the analysis result and are magnified by an amplification coefficient C_m. The C_m is defined as the ratio of yielding strength f_{yt} to the maximum stress f_{s_max} of confining steel, to approximate the ultimate confining stresses (i.e., the f'_{l1} and f'_{l2}) of the confined concrete elements. It should be noted that the magnified confining stresses are equivalent to the effective confining stresses denoted in the Mander model because the three-dimensional finite element

model can more realistically capture the confining stress distribution than an assumed one.
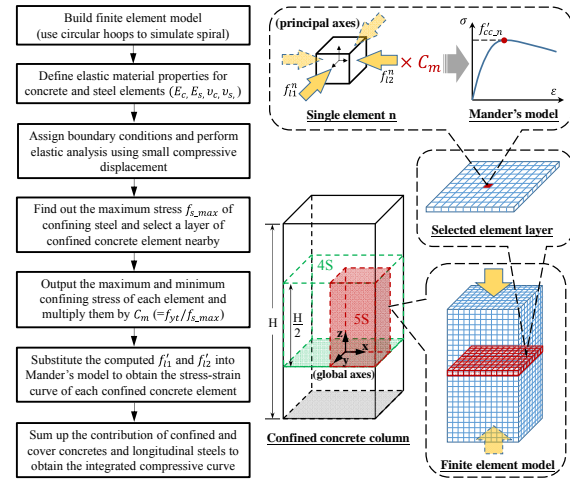

Figure 2: Flowchart and illustration of proposed simplified FEA method.

3 FINITE ELEMENT MODELING

3.1 Model Configuration

Two types of interlocking multi-spiral reinforcements, namely type 4S and type 5S, are considered in this research due to their superior confinement effects as mentioned in the introduction. Fig. 3 shows the selected configurations of these two types of columns, where the height of the column is 1200 mm with a cross section of 600 mm × 600 mm. Type 4S is composed of four identical interlocking spirals with a radius r_e = 180 mm. Type 5S consists of a central large spiral with a radius r_b = 210 mm interlocked with four small corner spirals having identical radius r_s = 105 mm. The layouts and bar sizes of the longitudinal reinforcements for the two columns, resulting in similar amounts of vertical reinforcements, are also designated in Fig. 3. On the other hand, the vertical spacing and bar size of transverse reinforcements vary according to different design scenarios, as given in later sections.
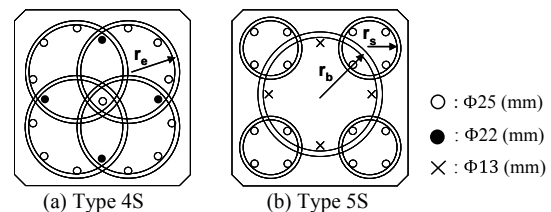

Figure 3: Configuration of interlocking multi-spiral column.

The finite element modeling and analyses were performed using the ANSYS general purpose finite element software. Given that the experimental axial stress-strain curves of the confined concrete columns were derived based on the displacement measurement within the middle-half column, only that part of the column was modeled in the finite element model, as illustrated in Fig. 2. This kind of modeling could also approximately neglect the boundary effects caused by the friction constraints between the testing machine and column specimen under compressive loading tests. Besides, due to the symmetry of the transverse reinforcement and based on the assumption that continuous spirals were simulated by discrete circular hoops, type 5S can be further modeled as one-fourth of the middle-half column, as shown in Fig. 2. As a result, only one-half and one-eighth of column specimens were modeled for types 4S and 5S, respectively. For the type 5S model, the boundary conditions $u(0, y, z) = 0$ and $v(x, 0, z) = 0$ were assigned to the symmetric planes of $x = 0$ and $y = 0$, respectively, where u and v are the nodal displacements along the global axes x and y, respectively, as designated in Fig. 2. For both types of models, the axial compression loading was applied by assigning $w(x, y, 0) = 0$ to the plane $z = 0$ and imposing an appropriate axial displacement $w(x, y, H/2) = w_z$ on the plane $z = H/2$, where w is the nodal displacement along the global axis z.

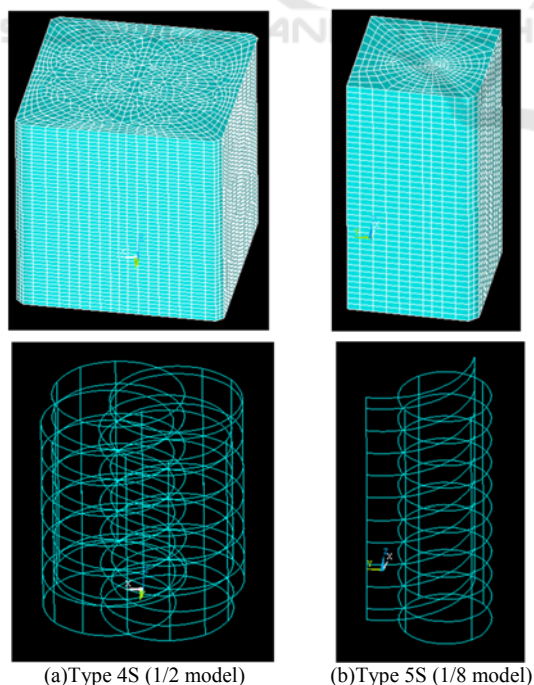(a)Type 4S (1/2 model)   (b)Type 5S (1/8 model)

Figure 4: Finite element models for types 4S and 5S columns.

In modeling the steel reinforcements of reinforced concrete members, three methodologies, namely the distributed, embedded, and discrete methods, are commonly used. To better capture the arching action between the levels of transverse reinforcements, the discrete method was adopted in this research. Both longitudinal and transverse reinforcing steel elements were explicitly constructed and attached to the adjacent nodes of concrete elements. Perfect bond between the concrete and steel was assumed; therefore, they shared the same nodal displacements at the concurrent nodes. An eight-node solid element and two-node link element were used for the concrete and reinforcing steels, respectively. The link element had axial strength but carried no bending stiffness. Fig. 4 shows the meshed finite element models for the types 4S and 5S columns where the element sizes were determined based on a mesh convergence analysis and the configuration of the reinforcing steels.

3.2 Steel Reinforcement

Considering that the finite element analyses in the proposed method was conducted within the elastic range, only fundamental material properties were needed. For both the longitudinal and transverse reinforcing steels, a Young's modulus E_s of 200 GPa and a Poisson's ratio v_s of 0.2 were used for modeling. The cross-section areas and vertical spacings of reinforcing steels were set according to their respective design requirements as presented in the next section. After the finite element analyses, the contribution of each element needed to be integrated to obtain the whole compression behavior of the column. At this stage of the calculation, an elastic-perfectly plastic stress-strain relation was used to approximate the axial compression behavior of longitudinal steels. This can be justified by the fact that after the transverse reinforcements yield, a reduction in the lateral restraint allows the buckling of longitudinal steels to occur, eliminating the strain hardening of steel.

3.3 Concrete Material Model

The Poisson's ratio of concrete v_c commonly ranges from 0.15 to 0.2, and $v_c = 0.17$ is used in this research. The modulus of elasticity of concrete E_c can be determined according to the formula suggested by ACI 318-14 (2014) as follows:

$$E_c = 4700\sqrt{f_c'} \text{ (MPa)} \qquad (1)$$

As mentioned previously, the magnified confining stresses (f'_{l1} and f'_{l2}) from the elastic finite element analysis results are utilized to compute the confined compressive strength f'_{cc} and the corresponding compressive stress-strain curve for each confined concrete element. The confined compressive strength f'_{cc} of concrete under multiaxial compressive stresses was derived by Mander et al. (1988) using an ultimate strength surface and was given in a plot relating the confining stresses and the confined strength. To aid numerical calculations, Chang and Mander (1994) proposed an approximate equation for the plot as follows:

$$K = \frac{f'_{cc}}{f'_c} = 1 + A\bar{x}\left(0.1 + \frac{0.9}{1 + B\bar{x}}\right) \quad (2)$$

where

$$\bar{x} = \frac{f'_{l1} + f'_{l2}}{2f'_c} \quad (3)$$

$$r = \frac{f'_{l1}}{f'_{l2}}, \quad f'_{l2} \geq f'_{l1} \quad (4)$$

$$A = 6.8886 - (0.6069 + 17.275r)e^{-4.989r} \quad (5)$$

$$B = \frac{4.5}{\frac{5}{A}(0.9849 - 0.6306e^{-3.8939r}) - 0.1} - 5 \quad (6)$$

In addition, the compressive strain ε_{cc}, corresponding to f'_{cc} in the Mander model, is given by

$$\varepsilon_{cc} = \varepsilon_{co}\left[1 + 5\left(\frac{f'_{cc}}{f'_c} - 1\right)\right] \quad (7)$$

where f'_c and ε_{co} are the unconfined concrete strength and corresponding compressive strain, respectively, and the latter is assumed to be 0.002 in this research.

4 VERIFICATOIN WITH EXPERIMENTAL RESULTS

The axial compression test results from Yin et al., (2011; 2012) and Wang (2004) for rectangular concrete columns using type 4S and 5S reinforcements are used to verify the proposed simplified FEA method. Table 1 lists the design parameters and material properties of the tested columns while their cross-sectional configurations are given in Fig. 3. Four type 4S columns, with different volumetric ratios of transverse reinforcement (ρ_t) ranging from 1.47% to 4.5%, are

used to study the effect of the amount of transverse reinforcements on the compressive behaviors of columns. The ρ_t is defined as the ratio of the volume of the interlocking multi-spiral reinforcements to the gross volume of the column. In addition, four type 5S columns are used to study the effects of the amount of transverse reinforcements (ρ_t= 1.44% to 2.56%) as well as the design combination of large and small spirals (i.e., having the same volume ratio but different bar sizes and spacings such as Columns 5S3 and 5S4) on column behavior.

Table 1: Design parameters and material properties.

| Specimen | f'_c (MPa) | Transverse reinforcement | | | | Maximum strength | | Error (%) |
		Spacing (mm)	Size (mm)	f_{yt} (MPa)	ρ_t (%)	Experiment (MPa)	Proposed (MPa)	
4S1	43.9	75	Φ13	323.4	2.0	57.0	55.5	-2.70
4S3	39.5	50	Φ16	372.1	4.5	70.6	67.3	-4.71
4S4	43.9	65	Φ16	372.1	3.5	65.5	66.5	1.55
4S5	43.9	100	Φ13	323.4	1.47	50.4	52.8	4.81
5S1	38.6	50	Φ13	323.4	2.56	57.6	55.3	-4.03
5S3	39.5	70(b)	Φ16	372.7	2.2	55.2	54.0	-2.27
		70(s)	Φ13	323.4				
5S4	39.5	60	Φ13	323.4	2.2	53.5	53.2	-0.49
5S5	38.6	50	Φ10	313.9	1.44	49.7	49.6	-0.28

Note: (b) and (s) indicate the large and small spirals, respectively, for the type 5S column.

4.1 Type 4S Columns

Fig. 5 shows comparisons of the analytical and experimental axial compressive stress-strain curves for the four type 4S columns. The analytical result of each column is presented in terms of the axial strength contributions from the confined core concrete (denoted as f_{c_conf}, unconfined cover concrete (denoted as f_{c_unconf}, and longitudinal reinforcements (denoted as $f_{s\_\Phi25}$ and $f_{s\_\Phi22}$. The axial stress of the individual contributing components were calculated as the axial force divided by the gross column cross-sectional area; therefore, the summation of each contributing stress-strain curve is the total stress-strain curve of column. To identify the effect of the cover concrete on the compressive behavior of the column, two summation results with and without the inclusion of the cover concrete, $SFEA_{\_total}$ and $SFEA_{\_conf}$, respectively, are also given in the figures. The two summation results show that the cover concrete has significant influence on the initial stiffness of columns. In addition, the initial stiffness of the analytical result with the cover concrete match well with that of the experimental curve for the four columns, until a significant nonlinearity of the experimental curve occurs. Then, the experimental curve approximately lies between the two analytical curves with and without the cover concrete before these two analytical curves coincide. This phenomenon can be explained by the fact that,

as axial deformation increases, the cover concrete tends to spall off the confined core because of their different levels of lateral expansion. Moreover, the defects on the column construction and the boundary constraints of the testing machine could also affect the onset of cover spalling. As a result, the cover concrete is usually unable to achieve its maximum strength, as shown in Fig. 5.
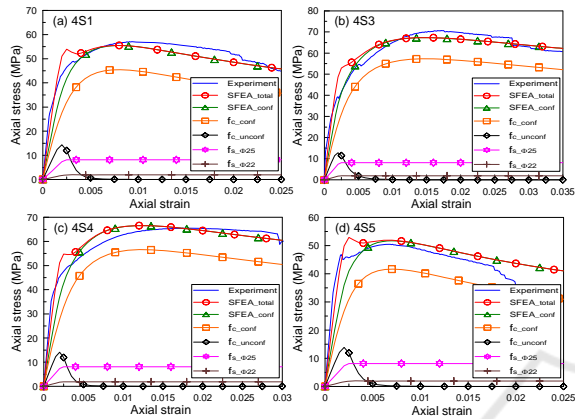

Figure 5: Comparison between experimental and analytical results for type 4S columns: (a) 4S1; (b) 4S3; (c) 4S4; and (d) 4S5.
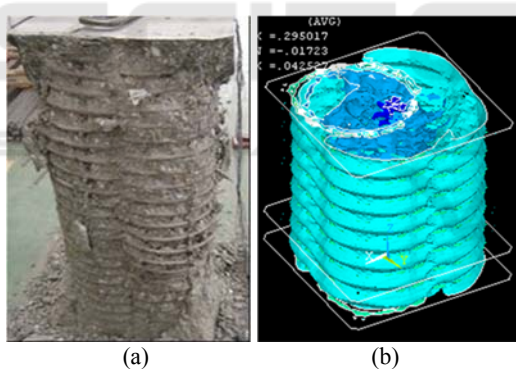

Figure 6: (a) Failure condition and (b) contour plot of equal maximum confining stress for Column 4S4.

In general, the proposed simplified finite analysis method can well predict the experimental axial stress-strain behaviors of the four columns in terms of the initial stiffness, the maximum axial strength, and the post-peak strength degradation behavior. As listed in Table 1, the maximum percentage of error in the maximum axial strength for the four columns is within 5%. This also indicates that the proposed method can effectively capture the effects of the amount of transverse reinforcements on the compressive behaviors of the type 4S columns. Fig. 6(a) shows the failure condition of Column 4S4 and Fig. 6(b) shows a contour plot of the equal maximum

confining stress from the finite element analysis of the corresponding column. It can be clearly seen from Fig. 6(b) that due to the arching action, the equal confining stress contour has decreasing sectional areas towards the middle of the two levels of confining steels, which conforms to the experimental observations shown in Fig. 6(a).

4.2 Type 5S Columns

Fig. 7 shows comparisons of the analytical and experimental axial compressive stress-strain curves for the four type 5S columns. In general, the proposed simplified method can satisfactorily capture the axial compression behaviors of the four columns despite the presence of some deviations in the prediction of the column initial stiffness and the maximum strength. The errors in the predicted maximum strength are within 4% as listed in Table 1. For these four columns, Column 5S4 has the best simulation results, where the experimental curve follows nearly the same slope as the analytical curve with cover concrete until an axial stress of around 32 MPa is reached, transfers between the two analytical curves with and without the cover concrete to approach the intersection of the two analytical curves, and then progresses closely with the descending branch of the analytical curves. The analytical results can appropriately reflect the positive trend of the increasing amount of transverse reinforcements on the maximum compressive strength, as observed in the test results.
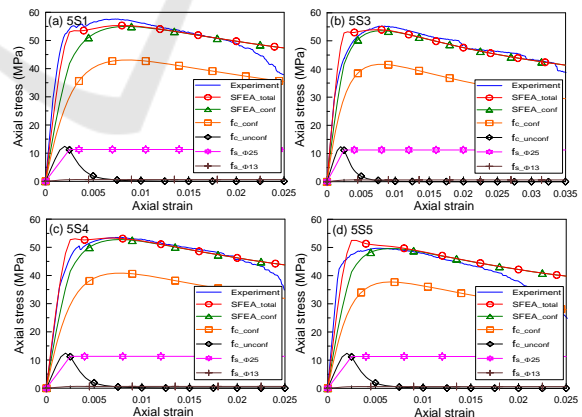

Figure 7: Comparison between experimental and analytical results for type 5S columns: (a) 5S1; (b) 5S3; (c) 5S4; and (d) 5S5.

In addition, under the same amount of transverse reinforcements, the effects of different design combinations of large and small spirals (i.e., Column 5S3 and 5S4) on the maximum compressive strength

can also be captured using the proposed method. Fig. 8(a) shows the failure condition of Column 5S3 while Fig. 8(b) shows the corresponding contour plot of equal maximum confining stress from the finite element analysis. As found in the type 4S column, the finite element analysis results could properly account for the arching actions formed between the two levels of confining steels.
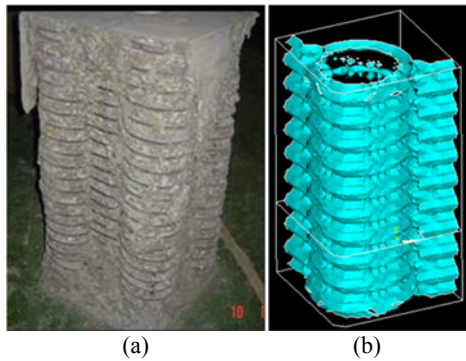

Figure 8: (a) Failure condition and (b) contour plot of equal maximum confining stress for Column 5S3.

5 PARAMETRIC STUDIES OF TYPE 5S REINFORCEMENT

Type 5S reinforcement is considered a promising method of transverse reinforcement for rectangular RC columns compared to type 4S due to the following reasons. The first is its superior confined behavior for the same amount of transverse reinforcement, as shown in Fig. 1. Secondly, type 5S reinforcement is beneficial for the assembly of the interlocking spiral cage, since the large spiral only needs to lap over a small spiral at each corner of the column. In contrast, each spiral of the type 4S reinforcement always has to interlock with the other three spirals. Finally, the small spirals of type 5S reinforcements allow the longitudinal steel of a column to be located much closer to the perimeter of the column than for type 4S, resulting in a greater flexural rigidity. Therefore, parametric studies were conducted by using the proposed method on type 5S reinforcement to investigate the influence of various spiral design parameters on the confinement efficiency. The dimensions of the column remained the same as those of the experimental studies mentioned above, but the radiuses (or diameters) of the large and small spirals were changed to produce different design combinations. A radius ratio (r_s/r_b), the ratio of the radius of the small spirals (r_s) to that of the large spiral (r_b), was used to define the geometry of the

interlocking spirals and hence its confined area (A_c). The A_c is the area enclosed by the outside edges of the interlocking spirals. As shown in Fig. 9, given a column section and a minimum depth (2 cm) of cover concrete, the confined area or the ratio (A_c/A_g) of the confined area to the gross area of the column section (A_g) increases as the radius ratio decreases. In the parametric studies, three radius ratios, namely r_s/r_b= 1/2, 1/3, and 1/4, were considered, resulting in A_c/A_g= 0.68, 0.74, and 0.80, respectively, where the first one is identical to the experimental ratio. In addition, the compressive strength of the unconfined concrete and the yielding strength of the spirals were assumed to be 34.3 and 274.4 MPa, respectively.
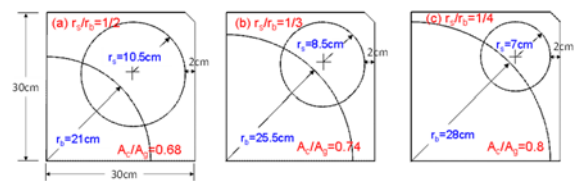

Figure 9: Geometries of type 5S reinforcements used in the parametric studies for: (a) r_s/r_b= 1/2; (b) r_s/r_b= 1/3; and (c) r_s/r_b= ¼.

5.1 Effect of the Amount of Large and Small Spirals

To investigate the effects of the amount of large and small spirals on the compressive strength of confined concrete, the proposed method was applied to columns with various combinations of large and small spirals for the three spiral radius ratios. The amount of spiral reinforcement is commonly represented by the volumetric ratio (ρ), which is the ratio of the spiral volume to the volume of core concrete confined by the spiral within a vertical spacing. In general, given a bar size and a vertical spiral spacing, the volumetric ratio of small spiral (ρ_s) is larger than that of large spiral (ρ_b) since the spiral volumetric ratio is inversely proportional to the spiral radius (or diameter). Therefore, the analytical cases of this section were devised in such a way that the ρ_b was fixed while the ρ_s was increased and greater than ρ_b. Moreover, the vertical spiral spacing was set to be 60 mm for all the analytical cases in this section. Figs. 10(a) to 10(c) show the relationships between the normalized compressive strength (f'_{cc}/f'_c) of the core concrete confined by the interlocking multi-spiral reinforcements and ρ_s associated with a specific ρ_b for r_s/r_b= 1/2, 1/3, and 1/4, respectively. When the ρ_b remains constant, the normalized compressive strength of the confined concrete is approximately proportional to the ρ_s for the three r_s/r_b cases. In

addition, the rate of increase of f_{cc}'/f_c' with increasing ρ_s (i.e., the slope of the line in the figures) tends to decrease as the r_s/r_b decreases. This can be attributed to the fact that for larger r_s/r_b, the small spiral has a greater contribution to the compressive strength based on the total confined area. On the contrary, when the ρ_s remains constant (i.e., ρ_s= 2.0% in the figures), the rate of increase of f_{cc}'/f_c' with increasing ρ_b (i.e., the difference of f_{cc}'/f_c' between different ρ_b in the figures) tends to increase as the r_s/r_b decreases.

According to ACI 318-14 (2014), the required amount of transverse reinforcement for the spiral confinement of a column is the greater of the following two equations:

$$\rho_{sp} = 0.45 \frac{f_c'}{f_{yt}} \left(\frac{A_g}{A_c} - 1 \right) \qquad (8)$$

$$\rho_{sp} = 0.12 \frac{f_c'}{f_{yt}} \qquad (9)$$

Eq. (8) is intended to ensure that the axial load capacity, based on the confined concrete strength f_{cc}' and the confined area A_c after cover concrete spalling, is not less than that based on the f_c' and A_g. Eq. (9) is intended to provide adequate curvature ductility at the potential plastic hinge regions of the column. For a column with A_c/A_g smaller than 0.79, which is nearly within the cases considered in the parametric study, Eq. (8) will govern the required amount of transverse reinforcement. Therefore, the code-required volumetric ratio of spirals according to Eq. (8) is inversely proportional to the A_c/A_g, and hence directly proportional to the r_s/r_b considered in this paper. Namely, the less the confined area, the greater confined concrete strength f_{cc}' associated with more transverse reinforcement is needed to compensate the spalling of the cover concrete. This implies that the value of f_{cc}'/f_c' should not be less than the reciprocal of A_c/A_g. Accordingly, for the cases of r_s/r_b= 1/2, 1/3, and 1/4, the minimum code-required ρ_{sp} are 2.62%, 1.95%, and 1.41%, which correspond to the minimum required f_{cc}'/f_c' of 1.47, 1.35, and 1.25, respectively. Figs. 10(a) to 10(c) also show the analytical results of columns with the code-required ρ_{sp} where the volumetric ratios of large and small spirals are both equal to the ρ_{sp}. It can be found that when the r_s/r_b= 1/2, the analyzed f_{cc}'/f_c' is almost identical to the code-required strength denoted by a dashed line. As the r_s/r_b decreases, it tends to produce a greater confined concrete strength than the code-required value.
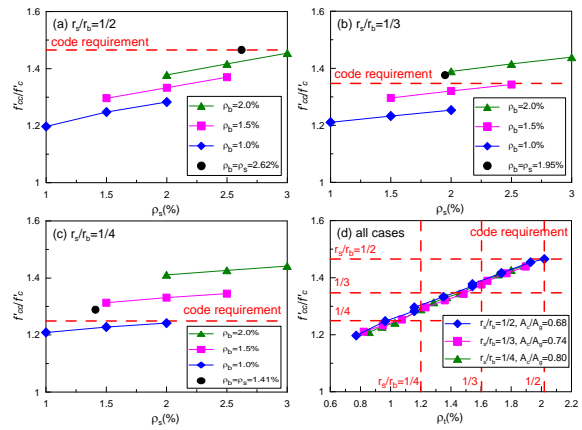

Figure 10: Effects of the amount of large and small spirals on normalized confined concrete strength for: (a) r_s/r_b=1/2; (b) r_s/r_b=1/3; (c) r_s/r_b=1/4; and (d) all cases.

5.2 Concurrent Yielding of Large and Small Spirals

The interlocking multi-spiral reinforcement consisting of one large and four small spirals was designed to collectively constrain the lateral expansion of the confined concrete core when subjected to axial loading. Therefore, failure of either the large or any small spiral would lead to the disintegration of the confining mechanism. In the general design cases mentioned above, namely the ρ_s being greater than ρ_b, the maximum steel stress of the large spiral (f_{sp_b}) is greater than that of the small spiral (f_{sp_s}), resulting in the failure or yielding of the large spiral before that of the small spiral. In addition, it was found that the ratio of f_{sp_b}/f_{sp_s} tended to decrease as the ratio of ρ_s/ρ_b decreased. Accordingly, the optimum design of the type 5S reinforcement was defined in this research such that the ρ_s/ρ_b ratio can cause the concurrent yielding of the large and small spirals to achieve economic design.

Figs. 11(a) to 11(c) show the relationships between the ratios of f_{sp_b}/f_{sp_s} and the ratios of ρ_s/ρ_b for r_s/r_b= 1/2, 1/3, and 1/4, respectively. For each plot in the figures, the ratio of ρ_s/ρ_b is varied based on a fixed ρ_b (i.e., ρ_b= 1.0%, 1.5%, or 2.0%). The ratio of f_{sp_b}/f_{sp_s} is approximately proportional to the ratio of ρ_s/ρ_b at a specific rate depending on the ratio of ρ_b. In addition, the three curves corresponding to different ratios of ρ_b nearly converge to the same point where the ratio of f_{sp_b}/f_{sp_s} is equal to one and the corresponding ρ_s/ρ_b, denoted as $(\rho_s/\rho_b)_{\_conc}$, are found to be

around 1.0, 0.8, and 0.7 for r_s/r_b= 1/2, 1/3, and 1/4, respectively. This indicates that, to achieve concurrent yielding of the large and small spirals, the ratio of $(\rho_s/\rho_b)_{\_conc}$ needs to be decreased when the ratio of r_s/r_b decreases.
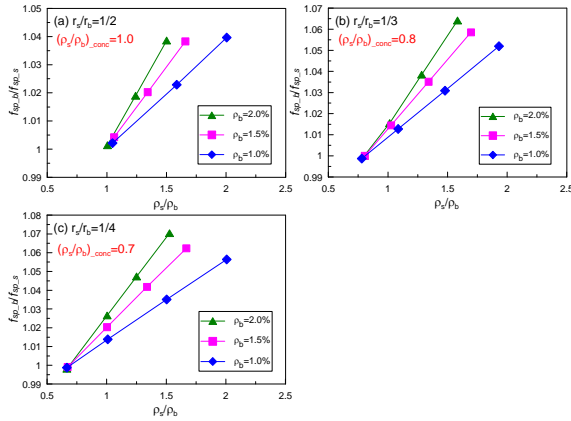

Figure 11: Relationships between f_{sp_b}/f_{sp_s} and ρ_s/ρ_b for: (a) r_s/r_b=1/2; (b) r_s/r_b=1/3; and (c) r_s/r_b=1/4.

5.3 Effect of Vertical Spiral Spacing

To examine the effect of the vertical spacing of the spiral on the compressive strength of confined concrete, the vertical spacing was varied while keeping the volumetric ratios of the large and small spirals unchanged. The ρ_b and ρ_s both conformed to the minimum requirement according to Eq. (8) and had the values of 2.62%, 1.95%, and 1.41% for the ratios of r_s/r_b= 1/2, 1/3, and 1/4, respectively. Fig. 12(a) shows the relationship between the f'_{cc}/f'_c and the vertical spacing of spirals for the three r_s/r_b cases. It is shown that the f'_{cc}/f'_c decreases as the vertical spacing increases. This can be attributed to the fact that the larger the vertical spacing, the less effective lateral confinement can develop between the two levels of spirals due to the arching action. Moreover, the analytical results also show that the rate of decline in f'_{cc}/f'_c associated with increasing vertical spiral spacing is more severe for cases with larger r_s/r_b than those with smaller ones.

Fig. 12(b) further examines the analytical results in terms of whether they can satisfy the code-required minimum strength, namely $f'_{cc}/f'_c \times A_c/A_g \geq 1$. It can then be found that, to satisfy the minimum strength requirement, the vertical spiral spacings could not be greater than around 60 mm, 125 mm, and 200 mm for the ratios of r_s/r_b= 1/2, 1/3, and 1/4, respectively.
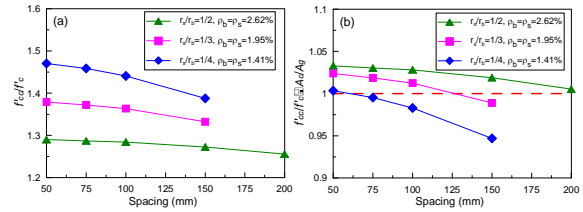

Figure 12: Effect of vertical spiral spacing on the compressive strength of columns in terms of: (a) f'_{cc}/f'_c and (b) $f'_{cc}/f'_c \times A_c/A_g$.

6 CONCLUSIONS

This study aims to propose a simplified finite element analysis method to analyze the axial compression behavior of rectangular concrete columns confined by interlocking multi-spiral reinforcement. The proposed simplified method utilizes the elastic finite element analysis to approximate the distribution and ultimate state of confining stress in each core concrete element, which is substituted into the Mander confined concrete model and then summed to obtain the integrated compressive curve of a column. Verification of the proposed method against test results of four type 4S and four type 5S columns shows good agreement between them. By using the proposed method, parametric studies focused on type 5S reinforcement were conducted to investigate the influence of various spiral design parameters on the confinement efficiency. Important conclusions can be drawn as follows:

- For the same amount of transverse reinforcement, a column with a lesser radius ratio r_s/r_b (or a larger confined area) can sustain approximately the same normalized confined concrete strength f'_{cc}/f'_c as its counterpart, resulting in a better axial load-carrying capacity and confinement efficiency.

- In order to achieve economic confinement design, the volumetric ratio of large spirals to that of small spirals (ρ_s/ρ_b), to have concurrent yielding of the large and small spirals, was found to be around 1.0, 0.8, and 0.7 for r_s/r_b= 1/2, 1/3, and 1/4, respectively.

- Given a minimum amount of spirals required by ACI 318-14, it was found that the vertical spacing of spirals could not be greater than around 60 mm, 125 mm, and 200 mm for the ratios of r_s/r_b= 1/2, 1/3, and 1/4, respectively, to fulfill the code-required minimum strength, namely $f'_{cc}/f'_c \times A_c/A_g \geq 1$.

ACKNOWLEDGEMENTS

REFERENCES

ACI Committee 318. 2014. Building code requirements for structural concrete (ACI 318-14) and commentary. *American Concrete Institute*, Farmington Hills, MI.

ANSYS. [Computer software]. *Swanson Analysis Systems*, Canonsburg, PA.

Caltrans (California Department of Transportation). 2003. Bridge design specifications. *Engineering Service Center, Earthquake Engineering Branch*, Sacramento, CA.

Cusson, Dj., and P. Paultre. 1995. "Stress-strain model for confined high-strength concrete." *J. Struct. Eng. 121* (3): 468-477.

Chang, G. A., and J. B. Mander. 1994. "Seismic energy based fatigue damage analysis of bridge columns: part 1- evaluation of seismic capacity." *Technical Report NCEER-94-0006*. University at Buffalo, New York, US.

Hoshikuma, J., K. Kawashima, K. Nagaya, and A. W. Taylor. 1997. "Stress-strain model for confined reinforced concrete in bridge piers." J. *Struct. Eng. 123* (5): 624-633.

Karabinis, A.I., and P. D. Kiousis. 1994. "Effects of confinement on concrete columns: plasticity approach." *J. Struct. Eng. 120* (9): 2747-2767.

Luccioni, B.M., and V. C. Rougier. 2005. "A plastic damage approach for confined concrete." *Computer & Structures. 83*: 2238-2256.

Mander, J. B., M. J. N. Priestly, and R. Park. 1988. "Theoretical stress-strain model for confined concrete." *J. Struct. Division. 114* (8): 1804-1826.

Malvar, L. J., K. B. Morrill, and J. E. Crawford. 2004. "Numerical modeling of concrete confined by fiber-reinforced composites." *J. Compos. Constr. 8* (4): 315-322.

Papanikolaou, V.K., and A. J. Kappos. 2009. "Numerical study of confinement effectiveness in solid and hollow reinforced concrete bridge piers: Methodology." *Comput. & Structures. 87*: 1427-1439.

Sheikh, S. A., and S. M. Uzumeri. 1982. "Analytical model for concrete confinement in tied columns." *J. Struct. Division. 108* (12):2703-2722.

Saatcioglu, M., and S. R. Razvi. 1992. "Strength and ductility of confined concrete." *J. Struct. Eng. 118* (6): 1590-1607.

Song, Z., and Y. Lu. 2011. "Numerical simulation of concrete confined by transverse reinforcement." *Comput & Concrete. 8* (1): 23-41.

Teng, J.G., Q. G. Xiao, T. Yu, and L. Lam. 2015. "Three-dimensional finite element analysis of reinforced concrete columns with FRP and/or steel confinement." *Eng. Struct. 97*:15-28.

Wang, P. H. 2004. "A study on new confinement configurations for rectangular concrete columns." [in Chinese.] *Master thesis*, Department of Civil Engineering, National Taiwan University, Taipei, Taiwan.

Yin. S. Y. L., J. C. Wang, and P. H. Wang. 2012. "Development of multi-spiral confinements in rectangular columns for construction automation." *J. Chinese Institute of Engineers. 35* (3): 309-320.

Yin. S. Y. L, T. L. Wu, T. C. Liu, S. A. Sheikh, and R. Wang. 2011. "Interlocking spiral confinement for rectangular columns." *Concrete International. 33* (12): 38-45.

Yu, T., J. G. Teng, Y. L. Wong, and S. L. Dong. 2010. "Finite element modeling of confined concrete-I: Drucker-Prager type plasticity model." *Eng. Struct. 32 (3): 665-679.*